Annals of Botany **117**: 79–95, 2016
doi:10.1093/aob/mcv150, available online at www.aob.oxfordjournals.org

ANNALS OF BOTANY
Founded 1887

Attack modes and defence reactions in pathosystems involving *Sclerotinia sclerotiorum*, *Brassica carinata*, *B. juncea* and *B. napus*

Margaret B. Uloth*[,1], Peta L. Clode[2], Ming Pei You[3] and Martin J. Barbetti[3,*]

[1]*School of Plant Biology,* [2]*Centre for Microscopy, Characterisation and Analysis and,* [3]*School of Plant Biology and The UWA Institute of Agriculture, Faculty of Science, The University of Western Australia, 35 Stirling Highway, Crawley, WA, 6009, Australia*
**For correspondence. E-mail martin.barbetti@uwa.edu.au*

Received: 8 April 2015 Returned for revision: 4 June 2015 Accepted: 19 August 2015 Published electronically: 29 September 2015

• **Background and Aims** Sclerotinia stem rot (SSR, *Sclerotinia sclerotiorum*) is a damaging disease of oilseed brassicas world-wide. Host resistance is urgently needed to achieve control, yet the factors that contribute to stem resistance are not well understood. This study investigated the mechanisms of resistance to SSR.
• **Methods** Stems of 5-week-old *Brassica carinata*, *B. juncea* and *B. napus* of known resistance were infected via filter paper discs impregnated with *S. sclerotiorum* mycelium under controlled conditions. Transverse sections of the stem and portions of the stem surface were examined using optical and scanning electron microscopy. The association of anatomical features with the severity of disease (measured by mean lesion length) was determined.
• **Key Results** Several distinct resistance mechanisms were recorded for the first time in these *Brassica*–pathogen interactions, including hypersensitive reactions and lignification within the stem cortex, endodermis and in tissues surrounding the lesions. Genotypes showing a strong lignification response 72 h post-infection (hpi) tended to have smaller lesions. Extensive vascular invasion by *S. sclerotiorum* was observed only in susceptible genotypes, especially in the vascular fibres and xylem. Mean lesion length was negatively correlated with the number of cell layers in the cortex, suggesting progress of *S. sclerotiorum* is impeded by more cell layers. Hyphae in the centre of lesions became highly vacuolate 72 hpi, reflecting an ageing process in *S. sclerotiorum* hyphal networks that was independent of host resistance. The infection process of *S. sclerotiorum* was analogous in *B. carinata* and *B. napus*. Infection cushions of the highly virulent isolate of *S. sclerotiorum* MBRS-1 were grouped together in dense parallel bundles, while hyphae in the infection cushions of a less aggressive isolate WW-3 were more diffuse, and this was unaffected by host genotype.
• **Conclusions** A variety of mechanisms contribute to host resistance against *S. sclerotiorum* across the three *Brassica* species. These complex interactions between pathogen and host help to explain variable expressions of resistance often observed in the field.

Key words: Sclerotinia stem rot, *Brassica carinata*, *B. juncea*, *B. napus*, white mould, histopathology, host–pathogen interaction, fungal infection, resistance, lignification, hypersensitive reaction, infection cushion.

INTRODUCTION

Sclerotinia stem rot (SSR) of brassicas is a damaging disease of oilseed rape and other oilseed brassicas in many parts of the world (Barbetti *et al.*, 2012). It is caused by the fungus *Sclerotinia sclerotiorum*, which has over 400 host species and affects a variety of plant parts (Boland and Hall, 1994). Only one study has specifically investigated the infection process of *S. sclerotiorum* on the stems of oilseed brassicas (Huang *et al.*, 2008), although the infection of other tissues of *Brassica napus*, such as leaves, petals, pollen and cotyledons (Jamaux *et al.*, 1995; Huang *et al.*, 1998, 2008; Garg *et al.*, 2010*c*) has been investigated. Additionally, detailed studies have been carried out on several other crop species that are hosts of *S. sclerotiorum*, such as potatoes and peas (Jones, 1976), bean (Lumsden and Dow, 1973; Abawi *et al.*, 1975; Tariq and Jeffries, 1986) and sunflower (Rodríguez *et al.*, 2004). Together, these studies show that the method by which *S. sclerotiorum* invades the host and establishes infection is similar across diverse susceptible hosts. The process involves germination of *S. sclerotiorum* ascospores followed by rapid growth of mycelium over the surface of the plant tissue. Approximately 24 h after growth has commenced, *S. sclerotiorum* begins to form appressoria and infection cushions. Hyphae from the infection cushions penetrate the plant using mechanical pressure, possibly assisted by the production of oxalic acid and polygalacturonase and other enzymes. The hyphae grow within the susceptible host, with mycelium ramifying from the penetration site through the cortex and sometimes into the vascular tissue of the host. Damage to the host tissue in the expanding lesion is catastrophic (Lumsden, 1979).

Huang *et al.* (2008) showed that infection processes on *B. napus* hypocotyls were largely similar to those on other plant parts, although larger infection cushions were found on the hypocotyl than on leaves. There was also evidence of some growth of *S. sclerotiorum* in the xylem of the hypocotyl 6 d post-infection (dpi).

While the infection process of *S. sclerotiorum* has been extensively examined, the information available deals almost exclusively with susceptible hosts while the resistance response has been little studied. This appears to be largely due to the lack of highly resistant genotypes available for investigation (Delourme *et al*., 2011). However, the discovery of high levels of resistance to stem infection in oilseed brassicas has now made investigation of the resistance response possible (Barbetti *et al*., 2013). Anatomical comparisons between resistant and susceptible Brassicaceae have so far been limited to a single study on *B. napus* cotyledons, which showed that while there was no difference between the germination of *S. sclerotiorum* ascospores on a moderately resistant variety 'Charlton' or susceptible 'RQ001-02M2', its growth was slow on the resistant variety (Garg *et al*., 2010*c*). The resistant genotype also suppressed formation of infection cushions, caused extrusion of protoplast from fungal hyphae and produced a hypersensitive reaction (HR). Although these findings in cotyledons are significant, such studies are not directly transposable to stems as there appears to be separate genetic control of stem resistance in seedlings versus adult plants (Zhao *et al*., 2006; Mei *et al*., 2012; Uloth *et al*., 2013*a*, *b*; Taylor *et al*., 2015). There is therefore a need to determine resistance mechanisms directly in oilseed *Brassica* stems, as stems are the host tissue most affected by SSR, relating directly to the major field losses caused by *S. sclerotiorum* (Li *et al*., 2006).

Oilseed *Brassica* breeders combine genetic material from a variety of *Brassica* species into breeding lines, which makes the level of resistance to *S. sclerotiorum* and mechanisms of resistance present in each species and their crosses a matter of great practical importance (Chen *et al*., 2010; Barbetti *et al*., 2014). We have therefore examined genotypes of known resistance from three species, namely *B. napus*, *B. juncea* and *B. carinata*, to determine whether their resistance reactions are similar. In addition, isolates of *S. sclerotiorum* differ in aggressiveness and pathotype but no attempts to reveal variation in infection processes between isolates of differing aggressiveness have been reported (Garg *et al*., 2010*b*; Ge *et al*., 2012). The comparison of highly and mildly aggressive isolates may reveal differences which could potentially lead to the development of novel methods to manipulate the pathogen and reduce disease.

In studies of SSR in field trials, a significant number of distinct stem lesion types have been observed on *Brassica* hosts with varying levels of resistance (Fig. 1). A consistent observation is that the stem lesions caused by *S. sclerotiorum* extend further longitudinally along the stem than radially (M. B. Uloth *et al*., unpubl. res.). In addition, dark 'shadows' extending well past the edge of the lesion are observed in many genotypes. These 'shadows' appear as sub-surface brown discoloration which runs longitudinally along the stem from the point of infection, under an intact cuticle/stem surface (Fig. 1B). Furthermore, the plant delimits lesions over time (Fig. 1C) in all but the most rampant infections (Fig. 1D). Studies into how *B. napus* limits the growth of *Leptosphaeria maculans* on its stem revealed a process of lignification, cambium formation and callose deposition at the edge of the lesion (Hammond and Lewis, 1986, 1987; Li *et al*., 2007*b*, 2008). Whether similar processes occur in association with infection by *S. sclerotiorum* remains unknown and the mechanisms governing the different types of lesions observed in the field need to be elucidated.

This work was carried out to (1) compare the infection processes of *S. sclerotiorum* between resistant and susceptible selections of *B. carinata*, *B. napus* and *B. juncea* in order to reveal resistance strategies employed by the host; (2) investigate and compare the infection process for *S. sclerotiorum* on *B. carinata* stems with that previously reported for *B. napus*; (3) investigate reasons for the preferential longitudinal extension of SSR stem lesions; and (4) establish whether differences in infection strategy occur between highly aggressive and mildly aggressive isolates of *S. sclerotiorum*.

In the course of the investigation it was noted that the cortex of the susceptible *B. carinata* genotype was consistently shallower than in the resistant genotype, with fewer cortical cell layers. Preliminary examination of the cortex in nine *Brassica* genotypes across *B. carinata*, *B. juncea* and *B. napus* (M. B. Uloth *et al*., unpubl. res.) and comparison with historical data on lesion lengths for these genotypes (Uloth *et al*., 2013*a*) supported the concept of a relationship between a lesser number of cell layers in the cortex and greater susceptibility to *S. sclerotiorum*. Therefore, an experiment was also conducted to test the hypothesis that *Brassica* genotypes with more layers in the cortex of the stem are more resistant to *S. sclerotiorum*.

MATERIALS AND METHODS

Host genotypes

Two separate experiments were conducted on the stages of the infection processes (Table 1). For Experiment 1, two selections of *B. carinata* were chosen as resistant and susceptible on the basis of their reaction to *S. sclerotiorum* in field trials (Uloth *et al*., 2013*a*) confirmed by several preliminary experiments in controlled environment growth rooms (Uloth *et al*., 2015*b*) (M. B. Uloth *et al*., unpubl. res.). *Brassica carinata* SMP3-82 from Pakistan was the most severely affected by *S. sclerotiorum* out of 108 diverse *Brassica* genotypes (mean lesion length = 155 mm), while *B. carinata* 054113 from Ethiopia was highly resistant (mean lesion length = 4·2 mm). In Experiment 2, 26 *Brassica* genotypes across *B. carinata*, *B. juncea* and *B. napus* (see Table 2) were selected using data from their performance in the Uloth *et al*. (2013*a*) field trial to provide a range of resistance levels. In particular, *B. napus* ZY006 from China was highly resistant in the field trial (mean lesion length = 7·1 mm), while *B. napus* YM04 from China was susceptible (mean lesion length = 41·6 mm), and these genotypes were chosen for more detailed examination.

S. sclerotiorum isolates

Two isolates of *S. sclerotiorum* were used in both experiments, MBRS-1 and WW-3. Both were collected from infected tissue of *B. napus* at sites where there was significant disease in an oilseed rape crop. MBRS-1 was collected from Mount Barker and WW-3 from the Walkaway region of Western Australia in 2004 (Li *et al*., 2006; Garg *et al*., 2010*b*). Cultures of these isolates were revived from original sclerotia stored in glass ampoules and subsequently refreshed as needed using air-dried mycelium-impregnated filter paper. Previous work has shown that MBRS-1 is highly virulent and represents pathotype

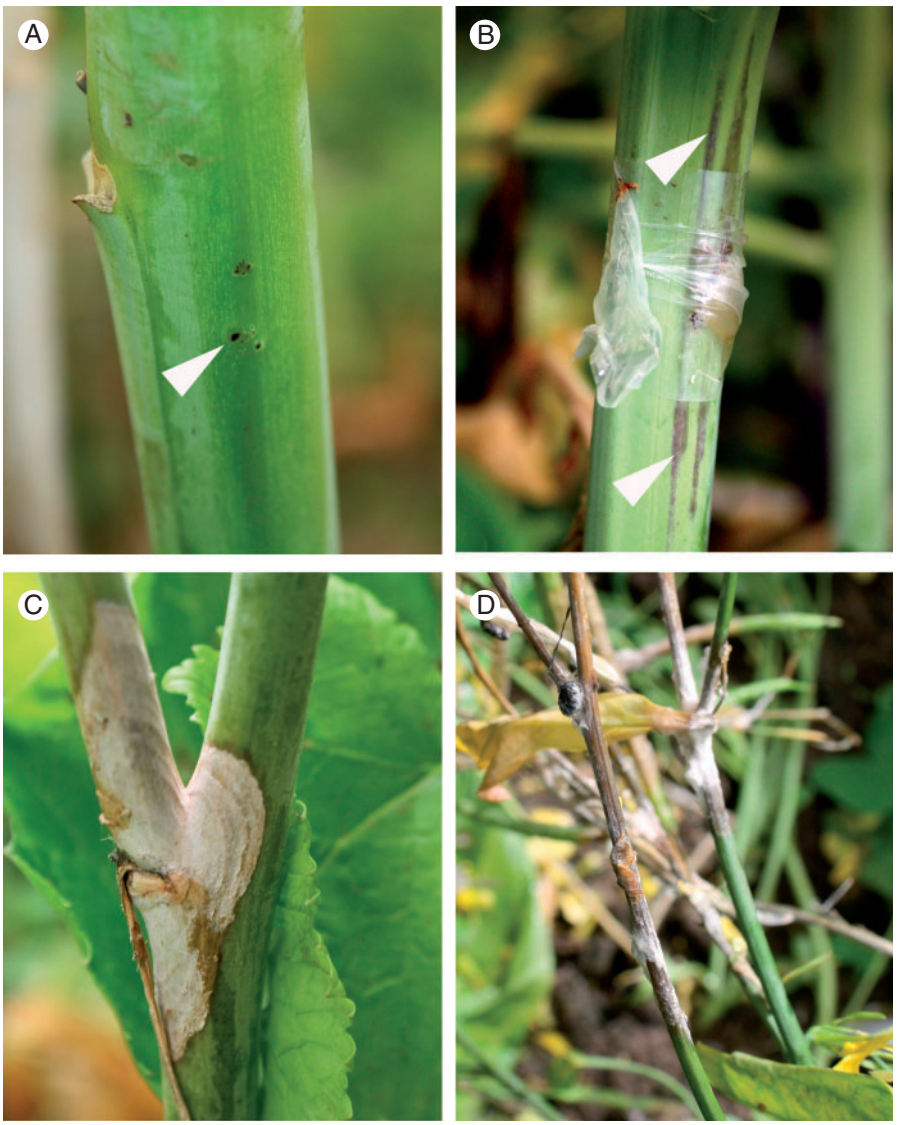

Fig. 1. Reactions by *Brassica* genotypes of varying susceptibility to infection by *Sclerotinia sclerotiorum* in a field trial. (A) Extreme resistance reaction at 21 dpi (arrowhead). (B) Stem inoculated with an *S. sclerotiorum*-infested agar plug, attached to the stem with Parafilm, showing sub-surface brown discoloration (arrowheads) caused by *S. sclerotiorum* infection running longitudinally along the stem from the point of inoculation at 21 dpi. (C) Moderately resistant reaction, showing zonate lesion at 21 dpi. (D) Highly susceptible reaction in *B. carinata* SMP3-82 at 21 dpi.

76, the prevailing pathotype in Western Australia, while isolate WW-3 is generally only weakly virulent and represents pathotype 10 in Western Australia (Ge *et al*., 2012; Uloth *et al*., 2015*b*).

Experiment 1: examination of the infection processes for a resistant and a susceptible genotype of B. carinata *by* S. sclerotiorum

Several microscopy techniques were used to compare the infection processes of *S. sclerotiorum* in the stems of resistant and susceptible 5-week-old *B. carinata* plants. Seed was sown into 35 × 29 × 6-cm trays, each having 48 individual cells filled with a pasteurized potting mix. Seedlings were transplanted after 3 weeks of growth in a controlled environment growth room, set to 22 ± 1 °C day and 18 ± 1 °C night, on a 12-h light–dark cycle, with light intensity of 400 µM m^{-2} s^{-1} into pots 14 cm in diameter (volume 1·7 L), with four plants per pot, and returned to the same growth room. Plants were grown for a further 3–4 weeks and were inoculated when stems were approx. 30 cm tall with a stem diameter up to 15 mm [growth stage between 2.05 and 3.5 on the Sylvester-Bradley scale (Sylvester-Bradley and Makepeace, 1984)].

Production of inoculum and plant inoculations were carried out as described by Uloth *et al*. (2015*b*). Inoculum was produced by placing five agar plugs from the actively growing margin of 3-d-old colonies of *S. sclerotiorum* grown on potato dextrose agar into 150 mL of liquid growth medium (per litre of water: 24 g potato dextrose broth and 10 g peptone). Cultures were shaken at 150 r.p.m. at 20 °C. After 3 d, actively growing mycelium was harvested by straining the broth through four layers of cheesecloth and washing with deionized water. The mycelium was macerated in the same liquid medium for 3 min

using a hand-held blender. The concentration of mycelia in the suspension was measured using a haemocytometer (Superior®, Marienfeld, Berlin, Germany), and adjusted to 1×10^4 fragments per millilitre by diluting with fresh growth medium. Round discs of filter paper 5 mm in diameter (Qualitative no. 2; Advantec MFS, Inc., Dublin, CA, USA) were added to the inoculum and allowed to stand for at least 15 min. The filter paper discs were applied to the stems of the plants above the first internode using Parafilm® as this technique mimics natural field infection from colonized flower petals (Uloth *et al*., 2015*a*). Plants were placed in controlled environment growth rooms at either 25/21 or 18/14 °C. Eighty-two pots of *B*. *carinata* SMP3-82 and 86 pots of *B*. *carinata* 054113 were inoculated. Half the pots were inoculated with each isolate and pots were randomized. The final number of plants examined was 321 for *B*. *carinata* SMP3-82 and 342 for *B*. *carinata* 054113. After inoculation, the plants were misted until leaves were visibly wet and relative humidity in the rooms was increased from 60 to 95 % night and 90 % day. Lesion length was measured at 72 h post-infection (hpi). Parafilm wrapping was removed and the length of the lesion on each stem (or length of the longest lesion if there were multiple lesions) was measured to the nearest millimetre with a ruler. Results were analysed using a two-factor analysis of variance using Genstat (14th edition, Lawes Agricultural Trust, Rothamsted Research, Harpenden, UK).

At 12, 24 and 72 hpi, sections of inoculated stems approx. 1·5 cm long were cut from the plants and immediately immersed in 2·5 % glutaraldehyde in phosphate-buffered saline. Further stem sections were immersed in acetic acid/ethanol/water (2 : 2 : 1 by volume) to decolourize tissues. Samples were held at 4 °C until required. Transverse sections 200 µm thick were cut from some of the stem sections using a Vibratome 3000 sectioning system fitted with razor blades. A series of sections were cut at known distances from the centre of the lesion. Sections were mounted in distilled water on glass slides and imaged with a Zeiss Axioplan microscope using both UV excitation and brightfield modes. Images were captured using a Zeiss Axiocam digital imaging system. Forty lesions were examined for each host × isolate combination. In other stems, the epidermis and the first few layers of cortical cells were removed from the inoculated area as a single layer using a scalpel. These samples were stained for 90 s in 0·05 % aniline blue, then rinsed in distilled water. Stained samples were placed in a drop of distilled water on a glass slide and observed under an Olympus BX51 microscope. Images were recorded using an Olympus DP71 digital photographic system with brightfield optics.

Small portions of infection sites, approx. 5 mm in length, were cut for observation of the stem surface using scanning electron microscopy (SEM). These were dehydrated in a graded series of ethanol (30, 50, 75, 100, 100 %) using a PELCO BioWave® microwave fitted with PELCO coldspot. For each change in ethanol solution, specimens were microwaved at 250 W for 40 s. Samples were then dried in a Polaron E3000 critical point drier, mounted on aluminium mounts with carbon tabs and coated with both 3 nm platinum and 10 nm carbon. Images were collected at 5 kV using a field emission scanning electron microscope (1555 VP-FESEM; Zeiss, Oberkochen, Germany).

Experiment 2: examination of the effect of the number of cortical cell layers, stem diameter and lignification on infection of Brassica *stems by* S. sclerotiorum

The average number of cell layers between the epidermis and the outermost vascular element (endodermis) was counted in the stems of 26 *Brassica* genotypes and related to stem diameter and the severity of infection 3 dpi. Lignification around the infection was also examined in stems at four time points after infection. Plants were grown in a controlled environment growth room set to 22 ± 1 °C day and 18 ± 1 °C night with a 12-h photoperiod. There were three pots each containing four plants for each genotype, and these were randomized in the growth room. Other conditions, growing methods and inoculation methods were as described for Experiment 1. Plants were inoculated when they were 5 weeks old. Growth stages of the different genotypes varied between 2·05 and 3·5 on the Sylvester-Bradley scale (Sylvester-Bradley and Makepeace, 1984) but all had an elongated stem suitable for inoculation. Parafilm wrapping was removed 3 dpi. The longest lesion on each stem was measured with a ruler to the nearest millimetre and 8–10 arbitrarily chosen stem sections were harvested for each genotype. Portions of stem approx. 80 mm long that encompassed the point of inoculation were cut, sealed in a plastic bag and held at 4 °C until observation. In total, 247 stems were included in the final analysis (numbers listed by genotype in Table 2), with a further 29 stems <4 mm in diameter discarded.

Transverse stem sections were cut with a razor blade by hand approx. 30 mm above the point of inoculation, and never within or immediately adjacent to a lesion. Sections were mounted in water on glass slides for observation with an Olympus BX51 microscope. The number of cell layers in the cortex between the endodermis and epidermis was counted (the endodermis and epidermis were not included in the count). The locations for counting were chosen arbitrarily, avoiding ridges and points of leaf attachment, as preliminary work showed little variation in the number of cell layers between repeated counts of a stem using this system (M. B. Uloth *et al*., unpubl. res.). The number of layers was counted in each stem. The diameter of the stems was measured using Vernier callipers to the nearest millimetre. The number of cell layers was analysed using a single-factor analysis of variance, then the relationship between the mean number of cell layers in the cortex, stem diameter, and mean lesion length for each genotype was determined using linear regression in GenStat (14th edition, Lawes Agricultural Trust).

The same stem portions were used to qualitatively assess anatomical responses at 3 dpi to infection by *S*. *sclerotiorum*, including lignification. Transverse sections were cut by hand using a razor blade at or near the centre of the lesion. At least five lesions were examined for each genotype. Sections were mounted in water and examined using an Olympus U-RFL-T burner with a mercury bulb as the fluorescence source, with a dichroic mirror DM400, excitation filter BP330-385 and barrier filter BA420. Other sections were cleared by placing them in a small amount of acetic acid/ethanol/water (2 : 2 : 1 by volume) solution in a lidded Petri dish. The Petri dish was then placed on a rack in a water bath set to 55 °C, not allowing water to enter the dish, and held for 10 min. Cleared sections were stained for 3 min using freshly prepared phloroglucinol-HCl (0·2 g

TABLE 1. *Stages of the infection process of* Sclerotinia sclerotiorum *on* Brassica carinata *stems following inoculation with filter paper discs impregnated with mycelium (Experiments 1 and 2)*

Infection stage	Infection process	Time observed (hpi)
1	Active growth of hyphae from disc onto stem	0–24
2	Formation of appressoria and infection cushions	24–48
3	Penetration of cuticle	24–48
4	Visible damage to stem	24–48
5	Secondary infections commenced. Growth of subcuticular hyphae in susceptible genotype	48
6	Extension of visible lesion into and along stem	48–72
7	Hyphae in lesion vacuolate. Lignification evident around lesions and in cortex	72
8	No viable hyphae visible on stem surface outside the lesion	96

phloroglucinol dissolved in 20 mL 20 % HCl) and examined for the presence of lignin (Gahan, 1984). Ten per cent of images obtained using fluorescence microscopy were cross-checked with stained images to confirm that the autofluorescence observed was due to the presence of lignin. Stems where surface discoloration was observed at the point of inoculation but no lesion had formed were selected and the epidermis and first few layers of cortical cells were excised and examined after staining with 0·05 % aniline blue as described in Experiment 1.

Following the harvest at 3 dpi, relative humidity in the growth room was reduced to 80 % during the day but maintained at 95 % at night and the remaining inoculated plants of *B. carinata* (SMP3-82, 054113) and *B. napus* (ZY006, YM04) continued to grow. More stems were harvested at 7, 14 and 19 dpi. At each time point, lesions in hand-cut transverse sections were examined as described above. At 19 dpi, lesion length for *B. carinata* SMP3-82 and 054113 was measured again with a ruler to the nearest millimetre. Mean lesion lengths were compared using the *t*-test function in Genstat.

RESULTS

Experiment 1: examination of the infection processes for a resistant and a susceptible genotype of B. carinata *by* S. sclerotiorum

Stages of infection. Sclerotinia sclerotiorum MBRS-1 and WW-3 successfully colonized and infected susceptible and resistant *B. carinata* stems. Mean lesion length for the susceptible *B. carinata* SMP3-82 was greater than for resistant *B. carinata* 054113 at 72 hpi [5·2 ± 0·2 mm ($n = 321$) and 2·6 ± 0·3 mm ($n = 342$), respectively, $P < 0{\cdot}001$]. Mean lesion length for *S. sclerotiorum* MBRS-1 was greater than for *S. sclerotiorum* WW-3 over both plant genotypes tested [4·9 ± 0·2 mm ($n = 317$) and 2·8 ± 0·2 mm ($n = 346$), respectively, $P < 0{\cdot}001$].

Several distinct stages were observed in the infection of *B. carinata* by *S. sclerotiorum* (Table 1). In the first stages of infection, hyphae grew in all directions from the filter paper disc onto and then along the stem of the host (Fig. 2A). Around 24 hpi, hyphal tips branched to form infection cushions. By 48 hpi, infection cushions were well established and secondary infections were forming (Fig. 2B). From qualitative observations, there were no obvious differences between host genotypes in the number or complexity of infection cushions. Subcuticular hyphae were frequently observed at the edge of lesions caused by MBRS-1 on the stems of *B. carinata* SMP3-82 (5/10 samples) (Fig. 2C), but were not seen in *Brassica carinata* 054113. At this stage lesions were visible to the naked eye as small black regions. *Sclerotinia sclerotiorum* infection then expanded into and along the stem. By 72 hpi the largest lesions (on *B. carinata* SMP3-82, but not on *B. carinata* 054113) were sunken and brown with a water-soaked appearance. White fungal growth was sometimes visible in the centre of these lesions. Most lesions on *B. carinata* 054113 were dry and black but remained visible. In *B. carinata* SMP3-82, the cytoplasmic contents of hyphae on the surface of the stem began to disappear by 72 hpi. Hyphae in the centre of lesions on both *B. carinata* genotypes became highly vacuolate or disintegrated completely (Fig. 2D), and by 96 hpi, hyphae were no longer visible on the surface of the stem outside the lesion.

Damage to vascular fibres in advance of lesion development. Sclerotinia sclerotiorum MBRS-1 preferentially targeted vascular elements in susceptible *B. carinata* SMP3-82 stems, frequently penetrating bundles of vascular fibres (Fig. 3C, E), or growing directly through the cortex to destroy vascular elements near the site of surface penetration (Fig. 3A). Damage was observed in the vascular fibres longitudinally up to 2·6 mm distal from the end of the lesion on the stem surface. In *B. carinata* 054113, vascular elements were sometimes damaged, but only where a substantial surface lesion had extended down to the edge of the vascular tissues. Damage to vascular fibres was never observed in advance of surface lesion development in *B. carinata* 054113, although some damage was evident in the cortex around the surface lesion (Fig. 3D, F).

Difference between highly aggressive and mildly aggressive isolates. Light micrographs showed that infection cushions of MBRS-1 were consistently more compact than those of WW-3 (Fig. 4). The structure of the infection cushions was not affected by the host genotype. Hyphae in the infection cushion of MBRS-1 were grouped together in dense parallel bundles (Fig. 4A, C), while the hyphae in the infection structures of WW-3 were more diffuse in their arrangement and less organized (Fig. 4B, D). Sometimes, bunched fungal hyphae of MBRS-1 entered the cortex as a group that strongly resembled an infection cushion and the cuticle around the entry point on the stem was depressed (Fig. 3B).

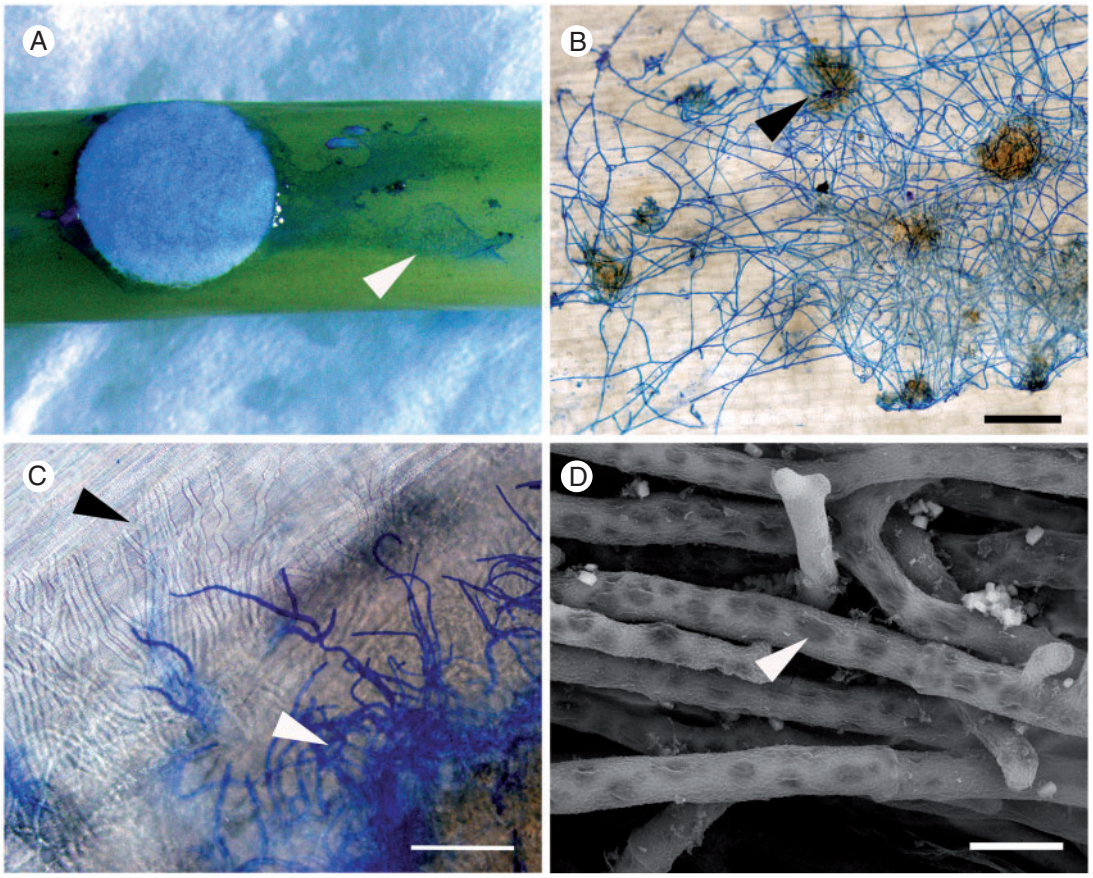

Fig. 2. Light and scanning electron micrographs showing disease progression caused by *Sclerotinia sclerotiorum* MBRS-1 (A–C) and WW-3 (D) on the stems of *Brassica carinata* following inoculation using colonized filter paper discs. (A) Extension of *S. sclerotiorum* along the surface of the stem of susceptible *B. carinata* SMP3-82 (arrowhead) at 24 hpi. (B) Established hyphal net on the surface of resistant *B. carinata* 054113 showing infection cushions (arrowhead) at 48 hpi. (C) Subcuticular hyphae visible in susceptible *B. carinata* SMP3-82 (black arrowhead) and surface hyphae (stained blue, white arrowhead) at 48 hpi. (D) Hyphae in the lesion and on the stem surface became highly vacuolated (arrowhead) by 72 hpi (susceptible *B. carinata* SMP3-82). Scale bars (B) = 500 μm, (C) = 66 μm, (D) = 10 μm.

Experiment 2: examination of the effect of the number of cortical cell layers, stem diameter and lignification on infection of Brassica *stems by* S. sclerotiorum

Effect of number of cell layers on lesion length. Lesions were severe in stems <4 mm in diameter regardless of genotype [mean lesion length at 72 hpi was 9·3 ± 0·3 mm for stems <4 mm ($n = 67$) and 5·6 ± 0·1 mm for stems ≥4 mm ($n = 181$)]. Therefore, data from plants with thin stems <4 mm were excluded from the analysis.

Mean lesion lengths at 3 dpi, the number of cell layers in the cortex and stem diameter for the 26 *Brassica* genotypes are shown in Table 2. The number of layers differed significantly between genotypes [$P < 0·001$, least significant difference (l.s.d.) = 1·9]. The lowest mean number of cells in the cortex was 6.6 for susceptible *B. carinata* SMP3-82, and the greatest was 16.1 for *B. napus* ZY005. Mean lesion length also differed significantly between the genotypes ($P = 0·01$, l.s.d. = 3·7). *Brassica juncea* #2 had the longest mean lesion length (9·1 mm) and *B. carinata* 054111 had the shortest (3·2 mm). There was a significant negative correlation between the mean number of cell layers in the cortex and mean lesion length across genotypes ($P < 0·001$, $r^2 = 0·434$, $n = 26$; Fig. 5). Mean stem diameter did not vary significantly between genotypes ($P = 0·372$).

Lesion length for B. carinata *SMP3-82 and 054113. Brassica carinata* SMP3-82 was among the most susceptible group of genotypes at 72 hpi (7·3 mm). Early infection on resistant *B. carinata* 054113 was unusually severe for this genotype, with lesions observed on approx. 30 % of stems. This contrasted with several preliminary experiments in which early infection on *B. carinata* 054113 was very mild and lesions appeared dry by 72 hpi. However, while mean lesion length at 19 dpi was 27·4 ± 8·0 mm for *B. carinata* SMP3-82, it was only 10·8 ± 1·0 mm for *B. carinata* 054113. A *t*-test confirmed the significance of this difference ($P = 0·05$; $t = 2·07$ on 36 d.f.), with strong evidence of different sample variances. *Brassica carinata* SMP3-82 had several very long lesions that encompassed the whole stem. Lesions as long as 230 mm were recorded and 15 % of the stems had lesions >40 mm. By contrast, the longest lesion on *B. carinata* 054113 was 31 mm. By 19 dpi, almost all lesions on *B. carinata* 054113 were dry in appearance.

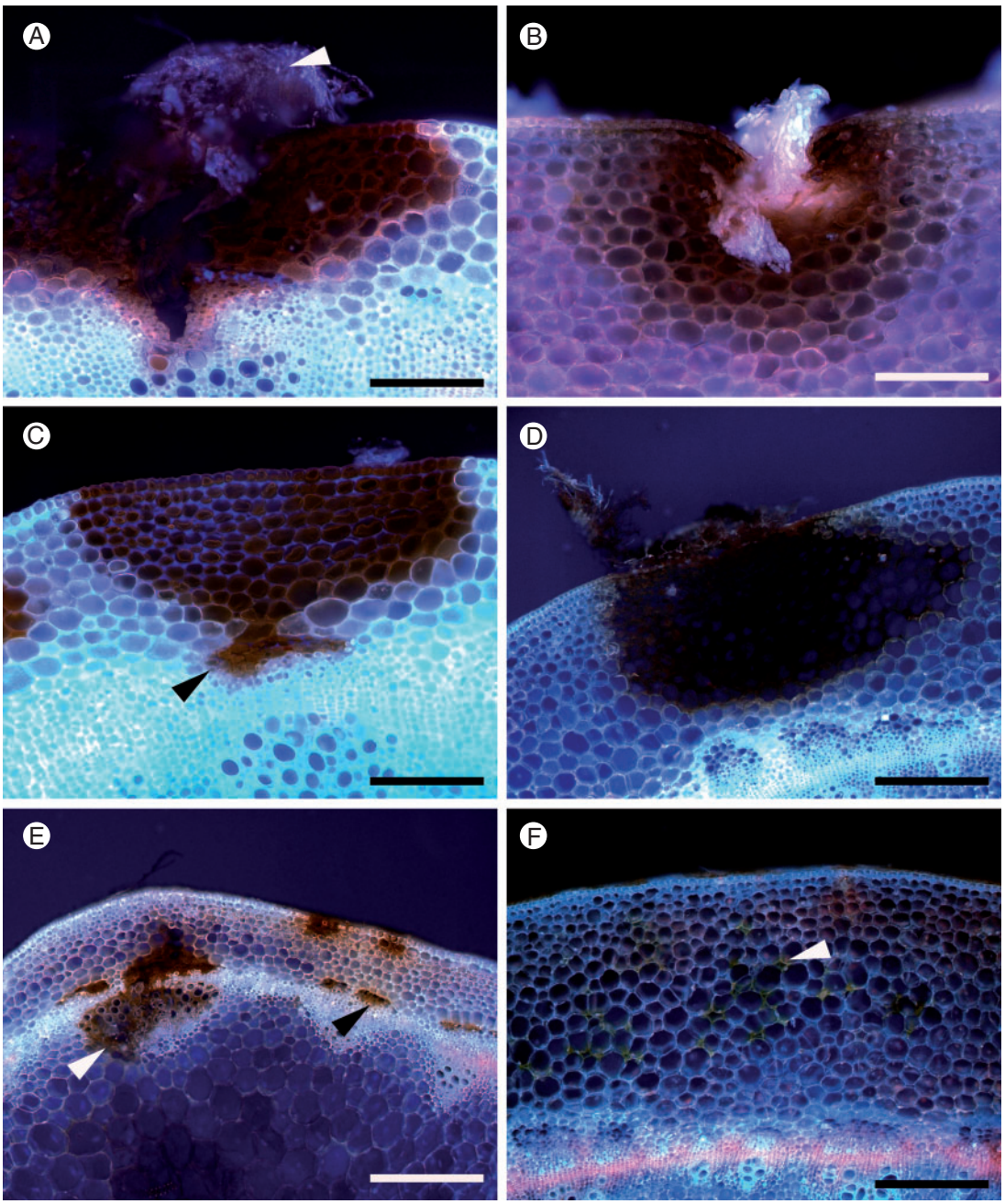

Fig. 3. Light micrographs of transverse sections of stems of susceptible *Brassica carinata* SMP3-82 (A, C, E) and resistant *B. carinata* 054113 (B, D, F) showing the development of lesions caused by *Sclerotinia sclerotiorum* MBRS-1 at 72 hpi. At the initial point of infection (A, B), approx. 1 mm away from the initial point of infection (C, D), and approx. 0·6 mm away from the edge of the externally visible lesion (E, F). (A) Susceptible *B. carinata* SMP3-82 centre of lesion with a fungal mass (arrowhead) showing numerous calcium oxalate crystals. Destruction of cells in the stem cortex and vascular system of the plant is evident. (B) Entry of *S. sclerotiorum* MBRS-1 into the stem of resistant *B. carinata* 054113. Stem cuticle around the entry point is depressed by the pressure of fungal penetration and fungal hyphae are evident in the stem, strongly resembling those in infection cushions. (C) *Sclerotinia sclerotiorum* from a surface lesion advancing to invade vascular fibres (black arrowhead). (D) Restriction of lesion to the stem cortex in a resistant host. (E) Destruction of vascular tissues, including bundles of vascular fibres (black arrowhead), and xylem (white arrowhead) in advance of the surface lesion. (F) Damage to cells in the stem cortex (arrowhead). Scale bars (A–C) = 100 µm; (D–F) = 200 µm.

Lignification in stem. Autofluorescence developed in diverse patterns in the stems of 26 *Brassica* genotypes tested in response to *S. sclerotiorum* infection. In general, the pattern of autofluorescence was identical to the pattern of red/pink coloration observed after staining with phloroglucinol, a stain which reveals areas of lignification (Fig. 6B, C). However, there were some exceptions to this, and in 4 % of samples, white autofluorescence was observed in a sample that did not stain with phloroglucinol. Autofluorescence of cell walls developed in different patterns in a range of *Brassica* genotypes. It was present in the

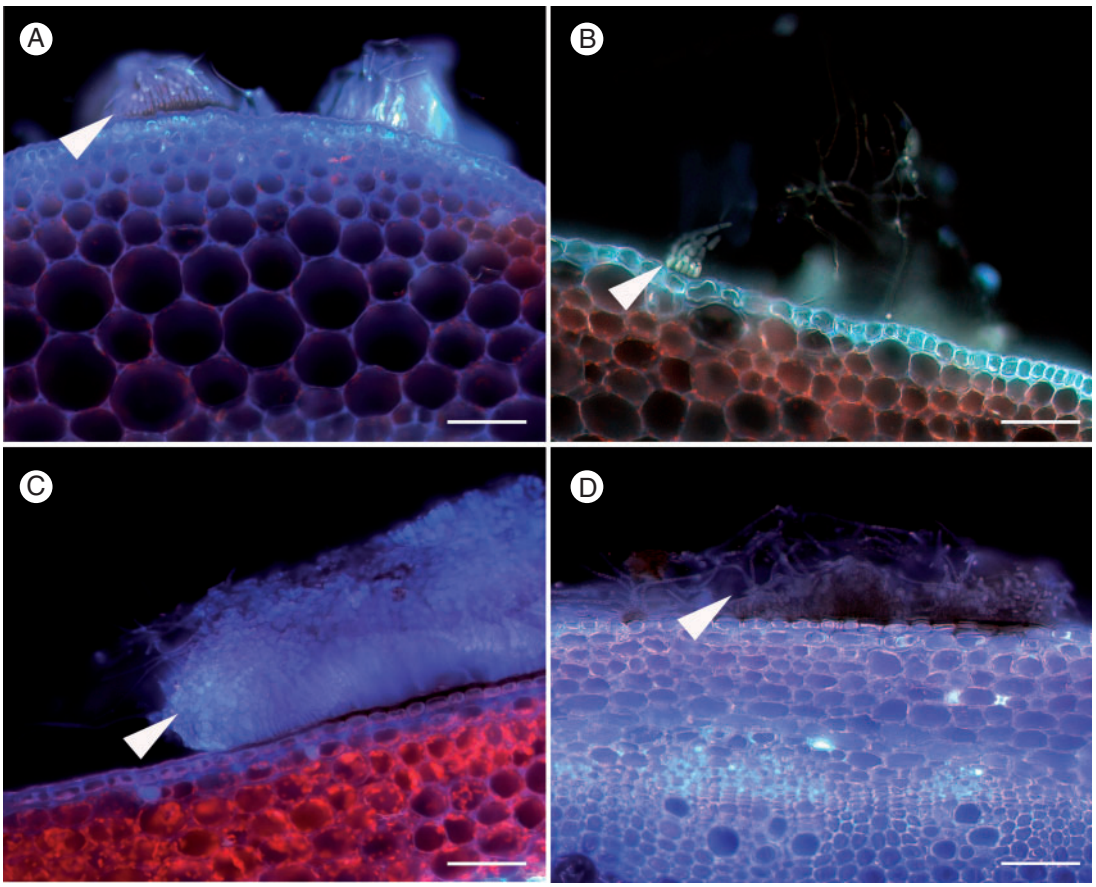

Fig. 4. Comparison of infection structures formed on susceptible *Brassica carinata* SMP3-82 by two isolates of *Sclerotinia sclerotiorum* with different levels of aggressiveness. (A) Isolate MBRS-1 (highly aggressive) infection cushions at 24 hpi (arrowhead), (B) isolate WW-3 (weakly aggressive) infection structure at 24 hpi (arrowhead), (C) isolate MBRS-1 dense infection cushion at 72 hpi (arrowhead), (D) isolate WW-3 diffuse infection cushion at 72 hpi (arrowhead). Scale bars (A–D) = 100 μm.

cortex around the edge of the lesion (Fig. 6A, B, C, F), in response to advancing mycelia (Fig. 6D), and in the endodermis, protecting the vascular tissues (Fig. 6A, C). Autofluorescence and phloroglucinol staining also developed in the cuticle in some genotypes (Fig. 6G, I).

Of the genotypes tested, the strongest autofluorescence at 3 dpi was in susceptible *B. napus* YM04 (Fig. 6A), which showed strong autofluorescence in the cuticle, around the borders of the lesion and also as a distinct barrier in the endodermis. By 19 dpi, the barrier around the surface lesion was extensive and intensive (Fig. 6B, C). Autofluorescence in other genotypes was less comprehensive and mostly comparatively weaker. Resistant *B. napus* ZY006 showed a strong autofluorescence reaction in the cortex to advancing mycelia (Fig. 6D), but there was no evidence of any defence reaction under brightfield illumination (Fig. 6E). *Brassica napus* YM18 also displayed strong autofluorescence in the cortex (Fig. 7B). In *B. napus* ZY006, a strong barrier had formed around the lesion by 19 dpi (Fig. 6F), but not in the endodermis (Fig. 6D, F). *Brassica napus* 'Mystic' developed a distinct barrier in the endodermis, but autofluorescence around the surface lesion was weak (Fig. 7A). The cuticle of *B. carinata* SMP3-82 fluoresced strongly near the edges of the surface lesion, but weakly around the lesion and in the cortex (Fig. 6G, I).

Brassica carinata 054113 generally showed little autofluorescence or lignification by 3 dpi (Fig. 8A, B), although in several samples a strong reaction to advancing mycelia in the cortex was observed. However, by 19 dpi, a distinct lignin layer developed, delimiting the surface lesion (Fig. 8C, D). While there was no clear relationship between the strength of autofluorescence at 3 dpi and lesion length, there was a trend for *Brassica* genotypes displaying strong autofluorescence in any part of the cortex to have smaller lesions (Table 2). In contrast, there was no evidence that autofluorescence in the cuticle was associated with increased resistance. Strong autofluorescence was not observed in the cuticle, cortex, or endodermis in the absence of *S. sclerotiorum* in any of the stems.

In genotypes that failed to stop the encroachment of *S. sclerotiorum* into the vascular system, fluorescence was reduced in colonized tissues (Fig. 6G), and when the same samples were viewed under brightfield illumination, damage to the stem was evident as dark discoloration (Fig. 6H). Infection sometimes resulted in breakdown within xylem bundles with a marked decrease in autofluorescence (Fig. 7C, D).

Discoloration of epidermal cell walls and HR. A typical HR (Ulloa and Hanlin, 2000), comprising dark brown/black dried spots or sometimes a slight discoloration of the stem surface,

TABLE 2. *Stem lesion length 3 dpi, the number of cell layers in the stem cortex and stem diameter, and presence of strong autofluorescence (AF) for 26* Brassica *genotypes (stems >4 mm in diameter) inoculated with* Sclerotinia sclerotiorum *MBRS-1 (Experiment 2); standard errors are indicated in parentheses*

Genotype name	*Brassica* species	Lesion length (mm)	No. of cortical cell layers	Stem diameter (mm)	Strong AF noted 3 dpi*	No. of plants (stem diameter >4mm)
054111	*B. carinata*	3·2 (0·8)	11·8 (0·3)	6·3 (0·6)	–	6
Mystic	*B. napus*	3·2 (0·6)	13·4 (0·5)	6·7 (0·6)	E	9
PI 197402	*B. carinata*	3·3 (0·6)	13·5 (1·8)	7·6 (1·4)	–	4
Charlton	*B. napus*	3·4 (0·7)	12·2 (0·5)	6·7 (0·7)	C	9
RT108	*B. napus*	3·7 (1·0)	13·0 (0·5)	7·3 (0·6)	C	9
ZY006	*B. napus*	3·8 (0·9)	11·4 (0·5)	7·2 (0·6)	C	9
06-P71–2	*B. napus*	3·9 (0·6)	11·4 (1·9)	7·2 (0·5)	E	8
YM14	*B. napus*	4·3 (0·8)	14·5 (0·8)	7·4 (0·6)	E	10
ZY005	*B. napus*	4·4 (0·5)	16·1 (1·3)	9·5 (0·8)	–	8
YM18	*B. napus*	4·9 (0·6)	13·0 (0·4)	6·6 (0·8)	E	8
JM06018	*B. juncea*	4·9 (0·6)	9·2 (0·5)	8·2 (0·6)	–	9
054103	*B. carinata*	5·1 (0·8)	10·7 (0·3)	7·4 (0·6)	–	9
PI 193459	*B. carinata*	5·4 (0·8)	12·0 (0·4)	7·3 (0·8)	C	8
YM04	*B. napus*	5·5 (1·1)	11·4 (0·4)	7·0 (1·2)	L, E, C	10
YM12	*B. napus*	5·5 (0·9)	12·8 (0·7)	6·0 (0·7)	–	8
BRA 926/81	*B. carinata*	5·7 (2·0)	9·3 (0·4)	7·0 (0·6)	–	7
054113	*B. carinata*	6·3 (1·4)	10·3 (0·4)	8·0 (0·7)	C	9
JO006	*B. juncea*	6·5 (0·9)	8·3 (0·4)	7·8 (0·5)	–	8
Montara	*B. juncea*	6·7 (1·2)	8·5 (0·5)	7·1 (0·7)	L	10
PI 360884	*B. carinata*	6·8 (1·1)	11·8 (0·7)	7·9 (0·3)	–	10
054106	*B. carinata*	6·9 (1·3)	12·1 (1·4)	7·4 (0·6)	–	7
SMP3–82	*B. carinata*	7·3(1·6)	6·6 (0·4)	7·3 (0·5)	–	9
JM06006	*B. juncea*	8·3 (2·4)	7·6 (0·4)	6·9 (0·6)	–	9
Xinyou 9	*B. juncea*	8·4 (1·7)	6·9 (0·5)	8·9 (0·5)	–	9
054104	*B. carinata*	8·6 (2·9)	12·6 (0·5)	8·0 (0·5)	–	9
B. juncea #2	*B. juncea*	9·1 (1·1)	7·4 (0·5)	6·7 (0·5)	–	7
Significance (P)		0·01	<0·001	0·372		
Least significant difference ($P \leq 0{\cdot}05$)		3·7	1·9	–		

*Lignification indicated by the presence of autofluorescence. Letters indicate strong autofluoresence was observed 'C' in cortex, 'L' around lesion or 'E' as a distinct barrier in the endodermis. '–' indicates no strong autofluorescence was observed.

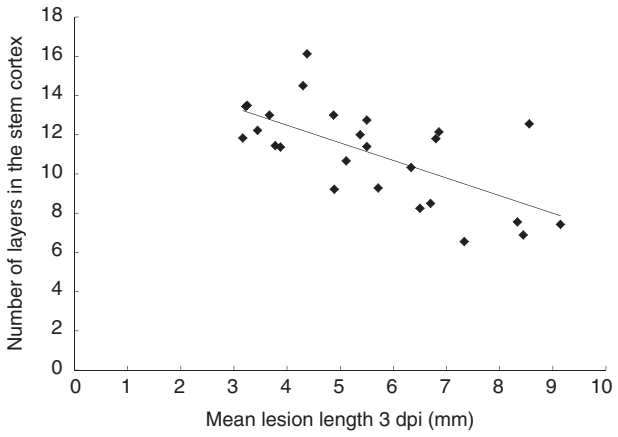

Fig. 5. Relationship between number of cell layers in the stem cortex for 26 *Brassica* genotypes and mean lesion length (mm) at 3 d post-inoculation (dpi) following inoculation with *Sclerotinia sclerotiorum* MBRS-1. Regression significant at $P < 0{\cdot}001$, $r = 0{\cdot}422$, $n = 26$.

indicated sites of failed infections on the stems of *B. carinata* and *B. napus* (Fig. 9). When decolourized stem surface tissues were observed under the microscope, there was often evidence of past *S. sclerotiorum* presence in the form of hyphal fragments and/or calcium oxalate crystals (Fig. 9A, B). It was noted that no autofluorescence was visible in the cell layers beneath these sites (Fig. 9C, E, F). In >95 % of samples, no further growth of *S. sclerotiorum* extended from these sites of discoloration within the epidermal layer (Fig. 9C, E, F). Infection sites that later developed into lesions could be distinguished by the presence of hyphae and/or cell damage in the cortex beneath the discoloured epidermis (Fig. 9D).

DISCUSSION

These studies are the first to define host–pathogen interactions involving *S. sclerotiorum* on stems of *B. carinata B. juncea* and *B. napus*. Comparison of resistant and susceptible genotypes of *B. carinata*, *B. napus* and *B. juncea* revealed a range of distinct mechanisms in *Brassica* stems associated with their relative ability to resist infection by *S. sclerotiorum*. Specific mechanisms defined in *Brassica* stems for the first time include HR, lignification within the stem cortex and/or around the edges of lesions, and a greater number of host cortical cell layers. Reasons for the preferential longitudinal extension of SSR stem lesions were explained, and the involvement of extensive vascular invasion in severe stem disease caused by *Sclerotinia* was demonstrated. Differences in infection strategy between highly aggressive and mildly aggressive isolates of *S. sclerotiorum* were highlighted. Hyphae of the highly virulent isolate MBRS-1 were shown to group together in dense parallel bundles in the infection cushion compared with more diffuse

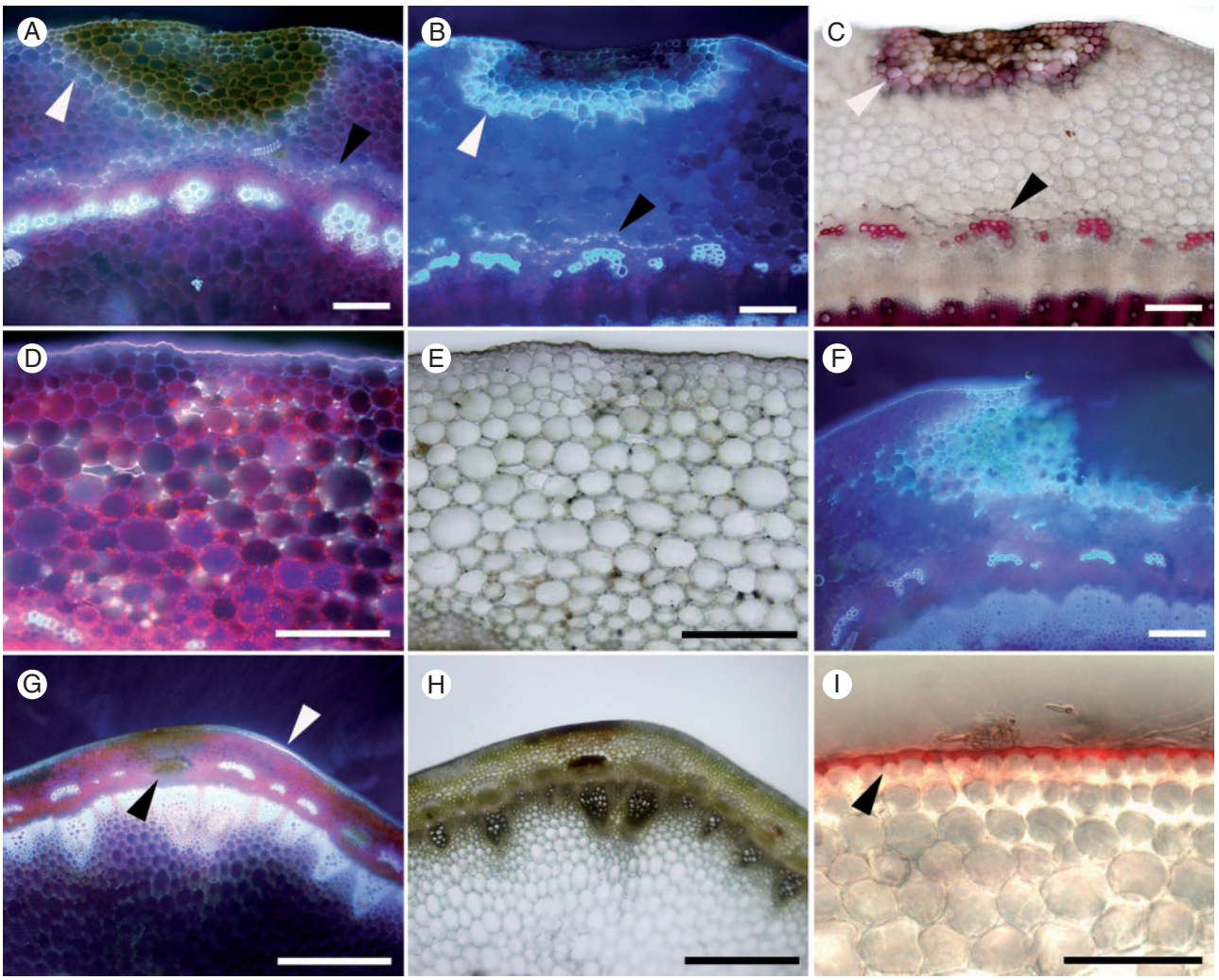

Fig. 6. Patterns of damage and lignification in transverse sections of *Brassica napus* stem at 3 or 19 d post-inoculation (dpi) following inoculation with *Sclerotinia sclerotiorum* MBRS-1. Images captured using fluorescence microscopy or phloroglucinol-HCL staining. (A) Susceptible *B. napus* YM04 showing strong autofluorescence (AF) surrounding lesion (white arrowhead) and formation of a lignin barrier in the endodermis (black arrowhead) at 3 dpi. (B) Susceptible *B. napus* YM04 at 19 dpi with very strong AF around the lesion (white arrowhead) and in endodermis (black arrowhead). (C) Susceptible *B. napus* YM04 at 19 dpi after phloroglucinol-HCl staining, showing wide band of lignification 'containing' the lesion (white arrowhead) and in the endodermis (black arrowhead). (D) Resistant *B. napus* ZY006 AF at 3 dpi showing strong AF in the cortex. (E) Resistant *B. napus* ZY006 at 3 dpi showing damage in the cortex (not stained). (F) Resistant *B. napus* ZY006 at 19 dpi showing very strong AF at the edge of a lesion. (G) Susceptible *B. carinata* SMP3-82 showing damage in vascular fibres (black arrowhead) and AF in the cuticle (white arrowhead) at 3 dpi. (H) Susceptible *B. carinata* SMP3-82 at 3 dpi (not stained). (I) Susceptible *B. carinata* SMP3-82 at 7 dpi showing lignification in the cuticle stained pink (arrowhead) following phloroglucinol-HCl staining. Scale bars (A, B, C, F) = 200 µm, (G, H) = 1 mm, (D, E, I) = 100 µm.

hyphae and less organized infection cushions of the weakly aggressive isolate WW-3. These findings demonstrate that the variable outcome of field stem infections and stem disease development is a consequence of complex interactions between several host resistance mechanisms and pathogen isolate characteristics. This study also demonstrated that infection processes on stems of *S. sclerotiorum* are analogous between *B. carinata* and *B. napus*.

Invasion of vascular system

Experiment 1 showed the movement of *S. sclerotiorum* into vascular fibres of susceptible *B. carinata* SMP3-82 soon after penetration, as well as growth along the vascular fibres or into and along the xylem. Experiment 2 demonstrated that genotypes where *S. sclerotiorum* extensively invaded the vascular system always had, relatively, very long lesions. *Sclerotinia sclerotiorum* preferentially targets the plant's vascular system, which provides not only nutrients but also a convenient conduit for rapid longitudinal growth. There have only been a few reports of *Sclerotinia* entering the xylem during infection of oilseed brassicas (Buchwaldt *et al.*, 2005; Huang *et al.*, 2008), common bean (Lumsden and Dow, 1973; Tariq and Jeffries, 1986) and clover (Prior and Owen, 1964), and this is the first time that the importance of entry to the vascular system has been demonstrated for any *Sclerotinia* species. In addition, entry of the fungus to the vascular system was observed earlier (3 dpi) than in the previous report for brassicas (6 dpi) (Huang *et al.*, 2008). Importantly, the current study was able to show the extent of vascular involvement in disease progression

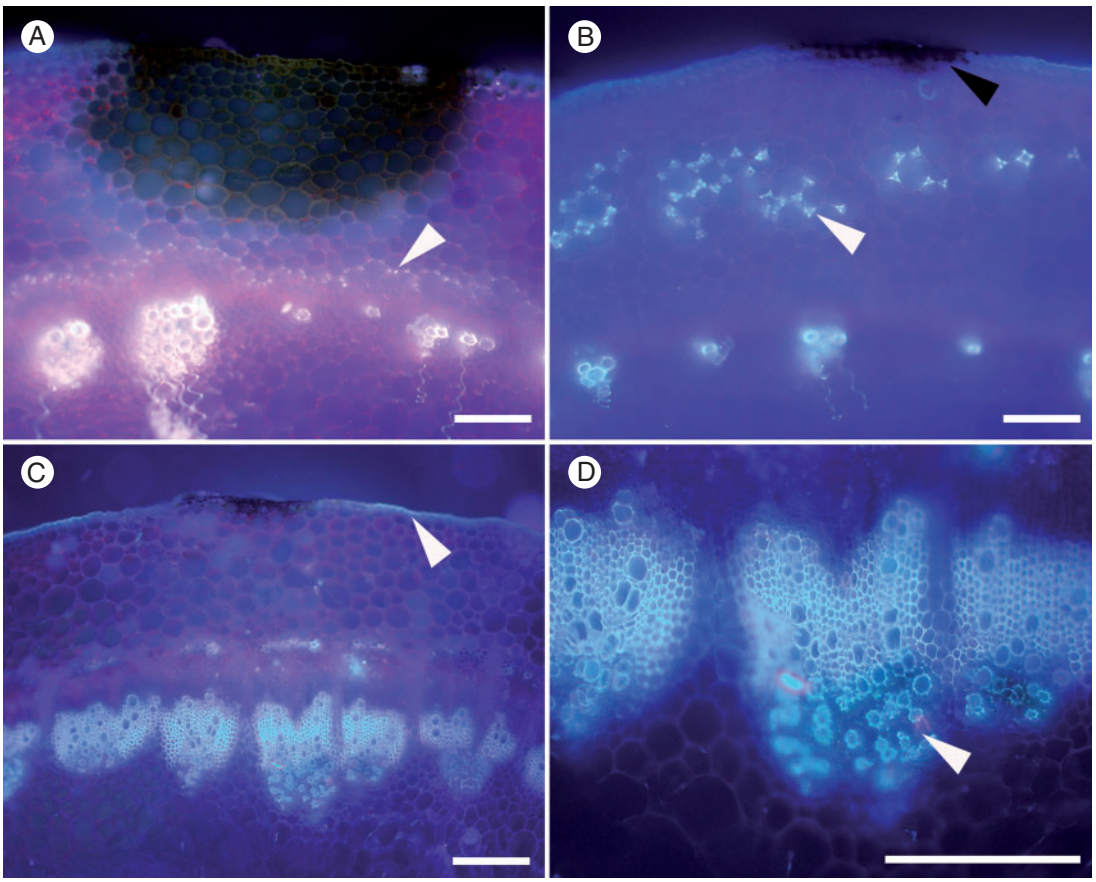

Fig. 7. Patterns of autofluorescence (AF) in transverse *Brassica* stem sections at 3 dpi following inoculation with *Sclerotinia sclerotiorum* MBRS-1. (A) Resistant *Brassica napus* Mystic showing AF barrier layer (arrowhead) only above the vascular system in the endodermis. (B) Strong AF reaction in stem cortex of susceptible *B. napus* YM18 at 3 dpi in response to hyphae growing through the cortex (white arrowhead). Hypersensitive reaction on stem surface (black arrowhead). (C) Susceptible *B. juncea* JM06006 showing weak AF present in cuticle (arrowhead) near the surface lesion and damage to xylem caused by *S. sclerotiorum*. (D) Susceptible *B. juncea* JM06006 showing greater detail from C, in particular showing damage to xylem bundles (arrowhead). Scale bars (A–D) = 200 µm.

for *S. sclerotiorum* because intact and elongated stems on plants approaching flowering were used, as opposed to the cotyledons (Garg *et al*., 2010*c*), hypocotyls (Huang *et al*., 2008) or detached plant parts (Jamaux *et al*., 1995) used in previous studies.

Subcuticular growth of S. sclerotiorum

The proliferation of prominent subcuticular hyphae helps *S. sclerotiorum* to rapidly exploit susceptible host tissues and extend growth up and down the stem. In Experiment 1, subcuticular hyphae were commonly present in the susceptible *B. carinata* SMP3-82 but not in the resistant *B. carinata* 054113, confirming the role of effective resistance in impeding this hyphal proliferation. A similar finding was previously made for *S. sclerotiorum* in *Phaseolus coccineus* (Lumsden, 1979), where resistant tissue posed a physical barrier to the fungus, while in the susceptible host infection hyphae were capable of rapid intercellular spread and development beneath the surface of the stem.

Utilization of the vascular system by *S. sclerotiorum* and/or extensive subcuticular growth helps explain the preferential longitudinal, rather than radial, expansion of SSR lesions. Damage associated with largely unimpeded movement of *S. sclerotiorum* through a stem's vascular system beneath intact surface tissues can be seen in the field with the naked eye (Fig. 1B) and explains why relative resistance to SSR in the Brassicaceae is best presented in terms of lesion length (Garg *et al*., 2010*a*).

Lignification in B. napus *and* B. carinata

This study provides the first strong evidence for a significant role for *S. sclerotiorum*-induced lignification in the stems of *B. carinata* and *B. napus*. Autofluorescence of cell walls indicated the presence of phenolic compounds that were laid down variously around lesions, within the cortex, in the cuticle and in a protective layer in the endodermis above the vascular elements of the stem when challenged by *S. sclerotiorum*. No autofluorescence was observed in these tissues in the absence of *S. sclerotiorum*. Successful staining with phloroglucinol-HCl of the same structures suggests strongly that the changes in cell-wall composition during infection by *S. sclerotiorum* were due to lignin deposition.

Lignin has often been proposed as an agent used by plants to defend against plant pathogens (Vance *et al*., 1980; Nicholson

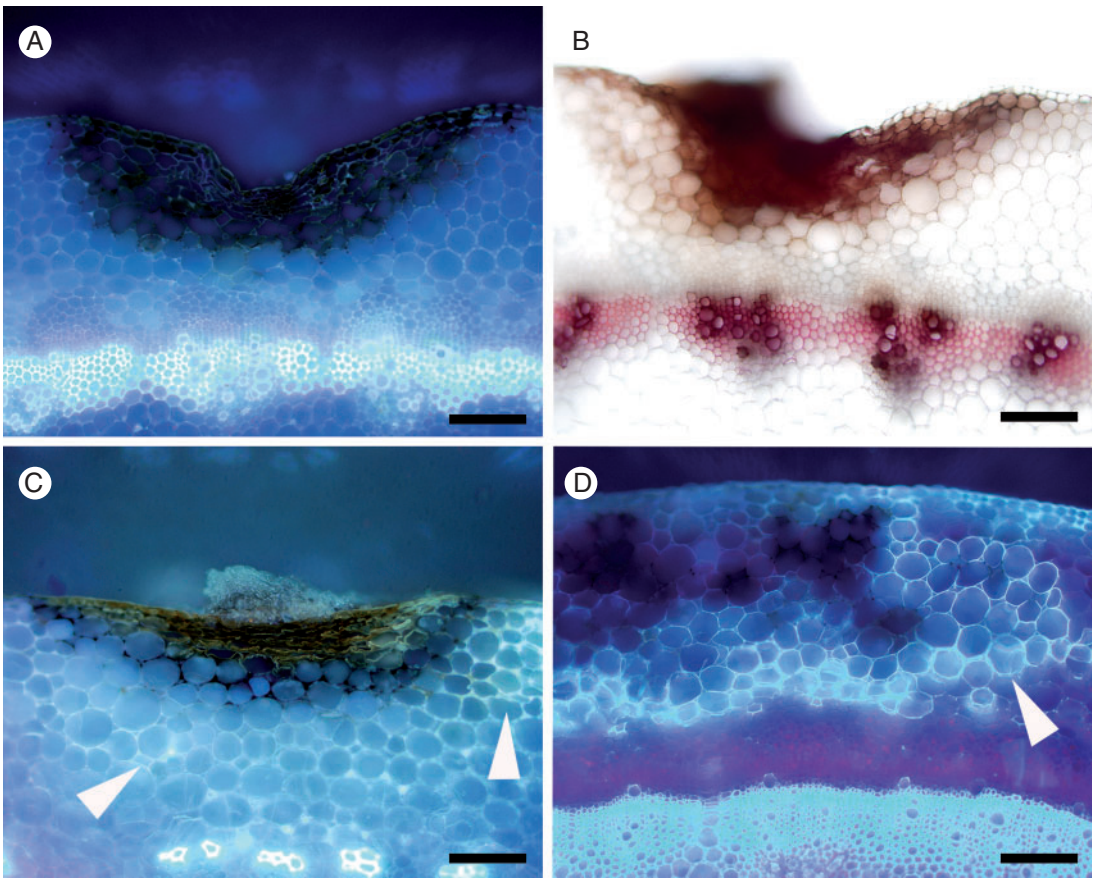

Fig. 8. Progression of lignification in resistant *Brassica carinata* 054113. (A) Minimal autofluorescence (AF) around the lesion at 3 dpi. (B) No lignification around the lesion at 3 dpi following phloroglucinol-HCl staining (lignin in xylem stained pink). (C) Developing AF around the lesion at 7 dpi (arrowheads). (D) Strong AF around the lesion at 19 dpi (arrowhead). Scale bars (A–D) = 200 µm.

and Hammerschimdt, 1992). It is thought to act as a physical barrier and to resist the diffusion of toxins produced by the pathogen (Dushnicky *et al*., 1998). Within the *Brassicaceae*, Eynck *et al*. (2012) presented evidence that a resistant selection of *Camelina sativa* produced more precursors of lignin biosynthesis and concluded that plant cell-wall strengthening plays a role in resistance to *S. sclerotiorum*. A gene involved in monolignol synthesis (BnaC.IGMT5.a) has recently been linked to a major resistance quantitative trait locus for *S. sclerotiorum* resistance in *B. napus* (Wu *et al*., 2013), supporting the current finding of lignification as an important mechanism of resistance to SSR. The lignification of cell walls within the stems of infected brassicas appears to impede the advance of *S. sclerotiorum* by not only stopping the extension of hyphae of *S. sclerotiorum* within the cortex, but also by building a protective 'containment' barrier around the edges of lesions. Previous work in *B. napus* has shown lignin deposition is an important resistance mechanism in response to infection by pathogens such as *L. maculans* (Li *et al*., 2007*a*, *b*) and *Verticillium longisporum* (Eynck *et al*., 2009). Of particular relevance are studies of *L. maculans* invasion of stems of *B. napus* (Li *et al*., 2007*b*), which showed post-penetration defence reactions including a HR, lignification, suberization and additional cambium formation in cultivars resistant to *L. maculans* that together impeded pathogen progress into the vascular tissues. Additional cambium formation was not observed with *S. sclerotiorum*.

The lignification reaction varied in location, strength and timing in each of the 26 *Brassica* genotypes tested. There was no direct relationship between the strength of the reaction and mean lesion length for a particular genotype, but there was a clear trend that genotypes showing strong lignification had shorter lesions 3 dpi. This suggests that while increased lignification is not always effective in providing early resistance to *S. sclerotiorum*, it can successfully curtail early growth of the pathogen where the expression of lignification is strong and rapid. It is likely that lignification becomes even more influential in the later stages of the infection process. This was best illustrated in *B. carinata* 054113 in Experiment 2, where lesions were completely surrounded by a thick layer of lignin by 14 dpi and were drying out, in spite of a substantial and seemingly uncontrolled infection at 3 dpi. The zonate appearance of many older lesions in the field (e.g. Fig. 1C) also suggests a role for lignification in delimiting *S. sclerotiorum*. This is in line with the findings of Hammond and Lewis (1986, 1987) for *L. maculans*. They described a series of attempts on the part of the plant to limit the spread of the fungus through lignification, which are overcome by the pathogen, leading to a similar zonate appearance of lesions. Further elucidation of the role of lignification in host defence against *S. sclerotiorum* is warranted. Clarification and classification of

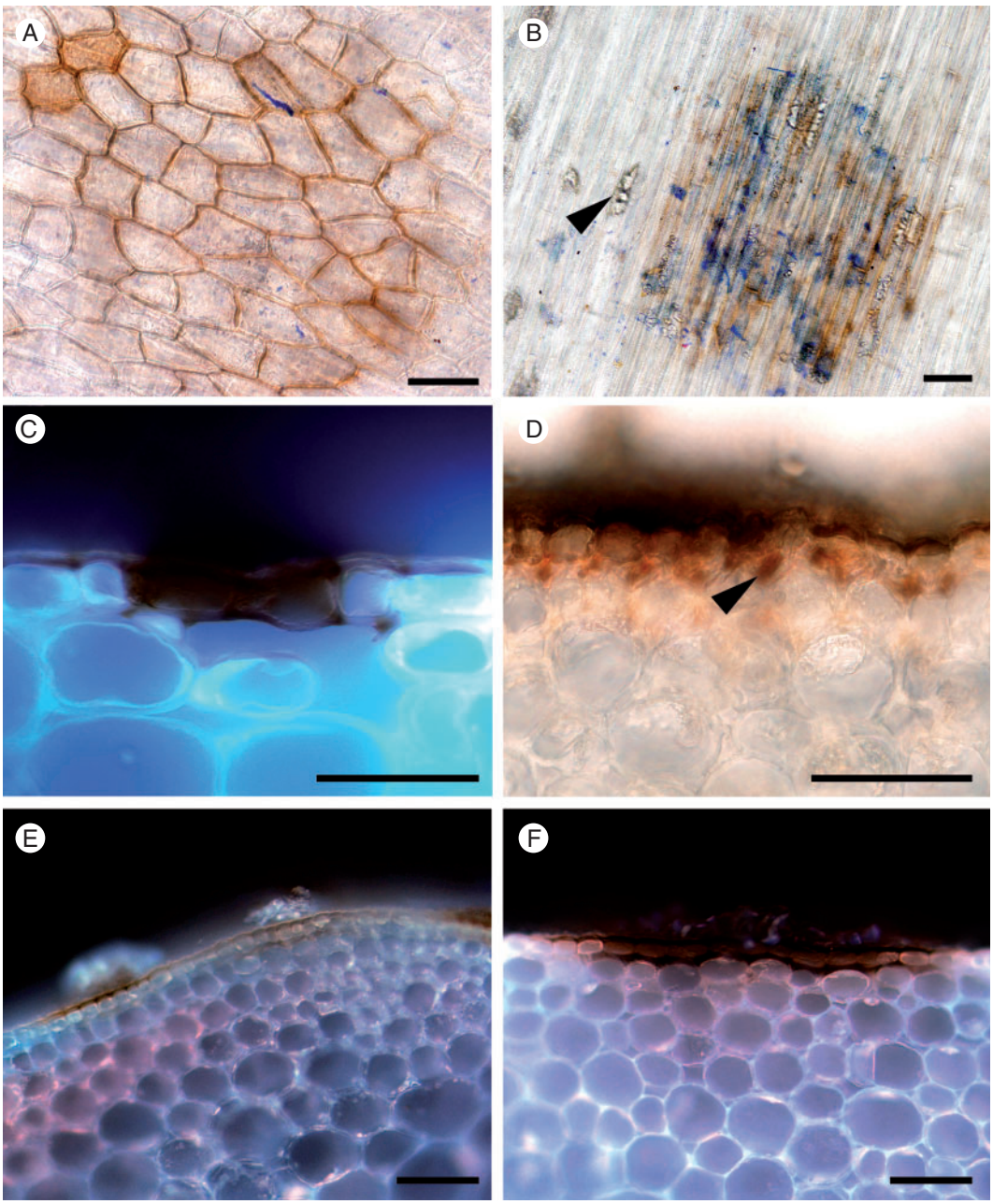

Fig. 9. Discoloration of epidermal cell walls after resistant and susceptible *Brassica carinata* and *B. napus lines* were challenged with *S. sclerotiorum* isolates MBRS-1 and WW-3 (A, B, C, E, F). Hypersensitive reaction (HR) at sites of failed infection on *Brassica* stems. (A) Resistant *B. carinata* 054113 at 3 dpi (WW-3). (B) Disintegrating hyphae, calcium oxalate crystals (arrowhead) and discoloration of cell walls at the site of an attempted infection on the stem of resistant *B. napus* ZY006 at 3 dpi (MBRS-1). (C) Discoloration of cell walls and cell death at site of a failed infection on resistant *B. carinata* 054113 at 3 dpi (WW-3). (D) Successful infection, with growth of subcuticular hyphae (arrowhead) in susceptible *B. napus* YM04 at 3 dpi in (MBRS-1). (E, F) Discoloration of cell walls and cell death at site of a failed infection on (E) susceptible *B. carinata* SMP3-82 at 3 dpi (MBRS-1) and (F) resistant *B. carinata* 054113 at 3 dpi (MBRS-1). Scale bars (A–F) = 50 µm.

lignification reactions from a wider range of brassicas may allow the future development of a rating scale for resistance that is measured by the lignification response.

Hypersensitive reaction

Strong evidence was provided in Experiments 1 and 2 that even susceptible *Brassica* genotypes can sometimes prevent entry of *S. sclerotiorum* using a HR. The HR is characterized by localized programmed cell death at the site of the attempted invasion by the pathogen and has been identified as the major defence reaction against other *Brassica* pathogens such as *L. maculans* (Li *et al.*, 2007*b*). Garg *et al.* (2008, 2010*c*) described a HR for *S. sclerotiorum* on *B. napus* and on *B. napus* and *B. juncea* containing one or more introgressions from weedy crucifer species. On the former, the expression of a HR

was secured by utilizing a weakly virulent isolate in combination with strict control of both inoculum concentration and environmental conditions (Garg *et al*., 2008). Sutton and Deverall (1984) also reported a HR in soybean affected by *S. sclerotiorum* at the site of fungal penetration, with the fungus restricted to cells showing the HR. With necrotrophic pathogens such as *S. sclerotiorum*, which can utilize dead cells as a nutrient source, it could be argued that plant cell death in the initial phases of the HR should promote fungal colonization of susceptible host tissue. However, it appears that there is a balance between promotion and destruction of the invading *S. sclerotiorum*, as argued by Williams *et al*. (2011). The lack of autofluorescence around the HR suggests that there was no further stimulation of the plant's defences after expression of the HR, except in the immediate surrounding cuticle. This autofluorescence reaction in the cuticle may be a response to the growth of *S. sclerotiorum* on the stem surface.

The observation of a HR in the *Brassica* genotypes examined is in agreement with information available from proteomic and biochemical studies of the resistance response of brassicas. These studies have revealed up-regulation of genes involved in the oxidative burst that are important in the initial phase of the HR, including evidence of the activation of salicylic acid and jasmonic acid-mediated defence responses and inhibition of H_2O_2 accumulation (Zhao *et al*., 2007, 2009; Wang *et al*., 2009, 2014; Rietz *et al*., 2012; Garg *et al*., 2013). Studies have also shown that protein production after infection and up-regulation of genes associated with defence, such as WRKY, zinc finger proteins and plant cell-wall-related proteins (Zhao *et al*., 2007) and phytoalexin production (Bennett and Wallsgrove, 1994), are all faster in resistant than in susceptible *Brassica* genotypes. Differences in the speed of the host response may help to explain the variable success of expression of the HR in highly and moderately susceptible *Brassica* genotypes. Where the HR is slow, it may be successful only in conditions that are not conducive to the pathogen, and fail in conditions that favour the pathogen. Similarly, the HR in a highly resistant genotype may not be successful in preventing infection in every case due to the balance between host and pathogen responses mentioned earlier (Williams *et al*., 2011). In fact, all *Brassica* genotypes in the current study were able to sometimes preclude significant colonization by *S. sclerotiorum* by invoking the HR. This ability may partially explain why inoculum levels are so important in determining the extent of disease development in the field (Clarkson *et al*., 2014). It follows that if only some of attempted infections are successful due to the HR, then a larger number of propagules will be needed to establish successful infection. In summary, our observations of the HR are consistent with the theory that infection by *S. sclerotiorum* always invokes a HR in *Brassica* stems; this sometimes prevents infection, but that at other times the programmed cell death of the HR instead helps the pathogen initiate a lesion. This would explain some of the observed variability in the response of brassicas to infection by *S. sclerotiorum* (Taylor *et al*., 2015). A more rigorous investigation of the HR on the stems of resistant and susceptible brassicas would be beneficial.

Variation in the expression of resistance was also seen in the early phases of infection within the stem, with resistant *B. napus* ZY006 having lesions as long as susceptible *B. carinata* SMP3-82 at 3 dpi in Experiment 2. In spite of this, by 19 dpi, the resistant variety had contained the lesions. The ability of *B. napus* ZY006 to reassert its control of the infection, even under conditions where *S. sclerotiorum* has successfully established an early infection, is likely to contribute to the genotype's consistently resistant phenotype in field trials and controlled environment experiments (Li *et al*., 2009; Ge *et al*., 2012; Uloth *et al*., 2013*a*, 2015*b*; Barbetti *et al*., 2014).

Number of cell layers in the stem cortex

The observation in initial imaging that a susceptible *B. carinata* genotype had fewer layers in the cortex than a resistant genotype led to an experiment comparing cell layers, stem diameter and lesion length for 26 *Brassica* genotypes. It is logical that the larger the number of cell walls the fungus has to breach, the slower its progress will be, and that extra cell layers would impede invasion of the vascular system. This was consistent with the study's results, and a significant negative correlation was found between the number of cell layers and the severity of infection. The influence of this parameter on *Sclerotinia* disease warrants study in other relevant host species.

A link between stem diameter and SSR resistance was proposed by Li *et al*. (2006) after a field trial in which genotypes with either a large ($>$ approx. 14 mm) or a small ($<$ 7 mm) stem diameter were more susceptible to infection. However, subsequent studies found little or no correlation between *Brassica* stem diameter and resistance (Li *et al*., 2007; Garg *et al*., 2010*a*). In the current study, mean stem diameter did not differ between *Brassica* genotypes. However, stems $<$ 4 mm in diameter were frequently catastrophically infected, and this is consistent with the finding of Li *et al*. (2006) that stems with the smallest diameters were more severely infected by *S. sclerotiorum*. It also implies that the level of resistance to SSR should be checked in *Brassica* genotypes tending towards particularly small stems before they are utilized in breeding programmes, especially where this is associated with few cell layers in the cortex.

Stage of infection process and ageing in the hyphal network

The techniques used in this study mimic natural infection processes, with the discs of filter paper impregnated with hyphae representing the infested petals from which the majority of stem infections occur in the field (Morrall and Dueck, 1982). The infection process and timing on *B. carinata* stems was similar to that reported on detached *B. napus* stems by Huang *et al*. (2008). A distinct ageing process was observed in the mycelium. Early in the infection process ($\leq$ 24 hpi), hyphae grew rapidly, were easily stained and full of opaque cytoplasmic contents, hyphal walls had a high level of integrity, and diffusion of hyphal protoplast materials onto the stem surface was not evident. However, after some hyphae penetrated the cuticle, integrity of the surface hyphae was lost, and by 72 hpi hyphae visible on the surface of the lesion were highly vacuolated. This pattern was evident across all genotypes and suggests that *S. sclerotiorum* has an organized hyphal network that follows a distinct 'ageing' process. The hyphal network commences with the growth of young hyphae on the stem surface, progresses to

penetration phase, and then to the exploitation of plant material and growth within the primary lesion. This leads to the production of a hyphal mass that can support extension along the host's stem and penetration into the interior of the stem. For hosts with a particularly narrow cortex, such as *B. carinata* SMP3-82, entry to the plant vascular tissues allows rapid access to these nutrient-rich tissues, and fosters rapid lesion expansion, with a longitudinal path unimpeded by constraints from cells/cell walls. Our observation of highly vacuolated older hyphae confirms the report of De Silva *et al.* (2009), who found that older hyphae were hard to image even with green fluorescent protein-transformed *S. sclerotiorum* due to their high level of vacuolation. The presence of heavily vacuolated hyphae in the surface lesions by 72 hpi suggests mobilization of resources to the advancing 'infection front' by *S. sclerotiorum* in the stem. Studies of the movement of radioisotopes through the hyphal network of a variety of fungi have shown that nutrients and organelles can be translocated from source to sink (Lindahl and Olsson, 2004), as the hyphal network ages. Translocation of nutrients from old to young hyphae of *Sclerotinia rolfsii* has also been demonstrated using radioisotopes (Wilcoxson and Subbarayudu, 1968). This process is analogous to the source/sink relationship between young and mature leaves of higher plants, where young developing leaves import photosynthetic assimilates exported by mature leaves (Fellows and Geiger, 1974). This mode of exploitation of resources by *S. sclerotiorum* hyphae in one area followed by transportation to the infection front suggests that if this process could be interrupted, then extension of the lesion and perhaps even subsequent production of sclerotia could be impeded. This provides a potential avenue through which control of *S. sclerotiorum* could be achieved.

Structure of infection cushions

The more aggressive isolate of *S. sclerotiorum* (MBRS-1) formed infection cushions that were more densely packed than those of the less aggressive isolate (WW-3), and this was independent of host. Infection cushions are known to vary in size and complexity according to the nutrition of the hyphae from which they are formed (Abawi *et al.*, 1975), and the mechanical resistance of the surface under attack (Tariq and Jeffries, 1984). *Sclerotinia sclerotiorum* relies in part on mechanical pressure to enable penetration of the host (Lumsden, 1979). It is possible that more compact infection cushions of MBRS-1 are able to exert more pressure than those of WW-3 and that this contributes to the greater aggressiveness of MBRS-1. That hyphae of MBRS-1 appear to be able to penetrate through the host surface layers *en masse*, in association with a depression of the surface layers which appears to have been caused by pressure exerted from the surface, supports this conclusion. Uloth *et al.* (2015*b*) recently showed that at high temperatures (28 °C), WW-3 can be equally as aggressive as MBRS-1. It would be interesting to determine whether this is at least partly due to the formation of more robust infection cushions by WW-3 at high temperatures.

Garg *et al.* (2010*c*) reported that the formation of infection structures was completely suppressed on the cotyledons of a resistant genotype of *B. napus*. On the stem, by contrast, there was no obvious difference in the number of infection cushions between resistant and susceptible genotypes. The distorted hyphae and extrusion of cell contents seen on resistant cotyledons (Garg *et al.*, 2010*c*) were also not observed. Although by no means definitive proof, these contrasting reactions support previous suggestions (Uloth *et al.*, 2013*a*) that different resistance mechanisms operate in *Brassica* stems, leaves and cotyledons, and also between seedlings and adult plants.

In conclusion, a range of resistance mechanisms in the stems of *B. napus* and *B. carinata* have been revealed, including: deployment of the HR; lignification within the stem cortex, in the endodermis and at the edge of lesions; and the influence of the number of cortical cell layers impeding *S. sclerotiorum* from reaching the vascular elements of the stem. These studies highlight the variable nature of the resistance reaction in the *S. sclerotiorum*/*Brassica* pathosystem. 'Susceptible' *Brassica* genotypes can sometimes impede infection processes in a limited way, and even 'resistant' genotypes can succumb where the pathogen isolate is highly virulent and environmental conditions are highly conducive. Further identification and control of factors affecting the expression of resistance to this devastating pathogen are essential to develop oilseed brassicas with high levels of reliable resistance, which would result in yield increases and reduction of pesticide use.

ACKNOWLEDGEMENTS

M.B.U. gratefully acknowledges the financial assistance of an Australian Postgraduate Award. Operational funding support for this research was provided by the School of Plant Biology, University of Western Australia (UWA), and by the Australia Research Council in conjunction with the Department of Agriculture and Food Western Australia (project LP100200113, 'Factors responsible for host resistance to the pathogen *Sclerotinia sclerotiorum* for developing effective disease management in vegetable brassicas'). Exceptional technical support from Mr Robert Creasy and Mr William Piasini in the UWA Plant Growth Facilities is also gratefully acknowledged. We acknowledge the facilities and assistance of the Australian Microscopy and Microanalysis Research Facility at the Centre for Microscopy, Characterisation and Analysis (CMCA), UWA, a facility funded by the University, State, and Commonwealth Governments. Able technical assistance from Mr John Murphy and Mrs Lyn Kirilak at the CMCA was particularly appreciated by M.B.U.

LITERATURE CITED

Abawi GS, Polach FJ, Molin WT. 1975. Infection of bean by ascospores of *Whetzelinia sclerotiorum*. *Phytopathology* **65**: 673–678.

Barbetti MJ, Banga SS, Salisbury PA. 2012. Challenges for crop production and management from pathogen biodiversity and diseases under current and future climate scenarios – case study with oilseed Brassicas. *Field Crops Research* **127**: 225–240.

Barbetti MJ, Uloth M, You MP, Liu SY, Banga SS. 2013. *Sclerotinia* on oilseed, forage and vegetable cruciferous crops—no longer an impossible disease to manage. In: *Proceedings of the 15th International Sclerotinia Workshop*, 20–24 August 2013, Wuhan, China. Wuhan, China: Huazhong Agricultural University, 62.

Barbetti MJ, Banga SK, Fu TD, *et al.* 2014. Comparative genotype reactions to *Sclerotinia sclerotiorum* within breeding populations of *Brassica napus* and *B. juncea* from India and China. *Euphytica* **197**: 47–59.

Bennett RN, Wallsgrove RM. 1994. Secondary metabolites in plant defence mechanisms. *New Phytologist* **127**: 617–633.

Boland GJ, Hall R. 1994. Index of plant hosts of *Sclerotinia sclerotiorum*. *Canadian Journal of Plant Pathology* **16**: 93–108.

Buchwaldt L, Li R, Hegedus DD, Rimmer SR. 2005. Pathogenesis of *Sclerotinia sclerotiorum* in relation to screening for resistance. In *Proceedings of the 13th International Sclerotinia Workshop*. Monterey, CA, 22.

Chen S, Zou J, Cowling WA, Meng J. 2010. Allelic diversity in a novel gene pool of canola-quality *Brassica napus* enriched with alleles from *B. rapa* and *B. carinata*. *Crop and Pasture Science* **61**: 483–492.

Clarkson JP, Fawcett L, Anthony SG, Young C. 2014. A model for *Sclerotinia sclerotiorum* infection and disease development in lettuce, based on the effects of temperature, relative humidity and ascospore density. *PLoS ONE* **9**: e94049.

De Silva AP, Bolton MD, Nelson BD. 2009. Transformation of *Sclerotinia sclerotiorum* with the green fluorescent protein gene and fluorescence of hyphae in four inoculated hosts. *Plant Pathology* **58**: 487–496.

Delourme R, Barbetti M, Snowdon R, Zhao J, Manazanares-Dauleux MJ. 2011. Genetics and genomics of disease resistance. In: D Edwards, J Batley, IAP Parkin, C Kole, eds. *Genetics, genomics and breeding of oilseed brassicas*. Boca Raton, FL: Science Publishers, 276–318.

Dushnicky LG, Ballance GM, Sumner MJ, MacGregor AW. 1998. The role of lignification as a resistance mechanism in wheat to a toxin-producing isolate of *Pyrenophora tritici-repentis*. *Canadian Journal of Plant Pathology* **20**: 35–47.

Eynck C, Koopmann B, Karlovsky P, von Tiedemann A. 2009. Internal resistance in winter oilseed rape inhibits systemic spread of the vascular pathogen *Verticillium longisporum*. *Phytopathology* **99**: 802–811.

Eynck C, Séguin-Swartz G, Clarke WE, Parkin IAP. 2012. Monolignol biosynthesis is associated with resistance to *Sclerotinia sclerotiorum* in *Camelina sativa*. *Molecular Plant Pathology* **13**: 887–899.

Fellows RJ, Geiger DR. 1974. Structural and physiological changes in sugar beet leaves during sink to source conversion. *Plant Physiology* **54**: 877–885.

Gahan PB. 1984. *Plant histochemistry and cytochemistry - an introduction*. London: Academic Press.

Garg H, Sivasithamparam K, Banga SS, Barbetti MJ. 2008. Cotyledon assay as a rapid and reliable method of screening for resistance against *Sclerotinia sclerotiorum* in *Brassica napus* genotypes. *Australasian Plant Pathology* **37**: 106–111.

Garg H, Atri C, Sandhu PS, *et al.* 2010*a*. High level of resistance to *Sclerotinia sclerotiorum* in introgression lines derived from hybridization between wild crucifers and the crop *Brassica* species *B. napus* and *B. juncea*. *Field Crops Research* **117**: 51–58.

Garg H, Kohn LM, Andrew M, Li H, Sivasithamparam K, Barbetti MJ. 2010*b*. Pathogenicity of morphologically different isolates of *Sclerotinia sclerotiorum* with *Brassica napus* and *B. juncea genotypes*. *European Journal of Plant Pathology* **126**: 305–315.

Garg H, Li H, Sivasithamparam K, Kuo J, Barbetti MJ. 2010*c*. The infection processes of *Sclerotinia sclerotiorum* in cotyledon tissue of a resistant and a susceptible genotype of *Brassica napus*. *Annals of Botany* **106**: 897–908.

Garg H, Li H, Sivasithamparam K, Barbetti MJ. 2013. Differentially expressed proteins and associated histological and disease progression changes in cotyledon tissue of a resistant and susceptible genotype of *Brassica napus* infected with *Sclerotinia sclerotiorum*. *PLoS ONE* **8**: e65205.

Ge XT, Li YP, Wan ZJ, *et al.* 2012. Delineation of *Sclerotinia sclerotiorum* pathotypes using differential resistance responses on *Brassica napus* and *B. juncea* genotypes enables identification of resistance to prevailing pathotypes. *Field Crops Research* **127**: 248–258.

Hammond KE, Lewis BG. 1986. Ultrastructural studies of the limitation of lesions caused by *Leptosphaeria maculans* in stems of *Brassica napus* var. *oleifera*. *Physiological and Molecular Plant Pathology* **28**: 251–265.

Hammond KE, Lewis BG. 1987. Variation in stem infections caused by aggressive and non-aggressive isolates of *Leptosphaeria maculans* on *Brassica napus* var. *oleifera*. *Plant Pathology* **36**: 53–65.

Huang HC, Kokko EG, Erickson RS, Hynes RK. 1998. Infection of canola pollen by *Sclerotinia sclerotiorum*. *Plant Pathology Bulletin* **7**: 71–77.

Huang L, Buchenauer H, Han Q, Zhang X, Kang Z. 2008. Ultrastructural and cytochemical studies on the infection process of *Sclerotinia sclerotiorum* in oilseed rape. *Journal of Plant Diseases and Protection* **115**: 9–16.

Jamaux I, Gelie B, Lamarque C. 1995. Early stages of infection of rapeseed petals and leaves by *Sclerotinia sclerotiorum* revealed by scanning electron microscopy. *Plant Pathology* **44**: 22–30.

Jones D. 1976. Infection of plant tissue by *Sclerotinia sclerotiorum*: a scanning electron microscope study. *Micron (1969)* **7**: 275–279.

Li CX, Li H, Sivasithamparam K, *et al.* 2006. Expression of field resistance under Western Australian conditions to *Sclerotinia sclerotiorum* in Chinese and Australian *Brassica napus* and *Brassica juncea* germplasm and its relation with stem diameter. *Australian Journal of Agricultural Research* **57**: 1131–1135.

Li CX, Li H, Siddique AB, *et al.* 2007. The importance of the type and time of inoculation and assessment in the determination of resistance in *Brassica napus* and *B. juncea* to *Sclerotinia sclerotiorum*. *Australian Journal of Agricultural Research* **58**: 1198–1203.

Li CX, Liu SY, Sivasithamparam K, Barbetti MJ. 2009. New sources of resistance to Sclerotinia stem rot caused by *Sclerotinia sclerotiorum* in Chinese and Australian *Brassica napus* and *B. juncea* germplasm screened under Western Australian conditions. *Australasian Plant Pathology* **38**: 149–152.

Li H, Kuo J, Barbetti MJ, Sivasithamparam K. 2007*a*. Differences in the responses of stem tissues of spring-type *Brassica napus* cultivars with polygenic resistance and single dominant gene-based resistance to inoculation with *Leptosphaeria maculans*. *Canadian Journal of Botany* **85**: 191–203.

Li H, Stone V, Dean N, Sivasithamparam K, Barbetti M. 2007*b*. Breaching by a new strain of *Leptosphaeria maculans* of anatomical barriers in cotyledons of *Brassica napus* cultivar Surpass 400 with resistance based on a single dominant gene. *Journal of General Plant Pathology* **73**: 297–303.

Li H, Sivasithamparam K, Barbetti M, Wylie S, Kuo J. 2008. Cytological responses in the hypersensitive reaction in cotyledon and stem tissues of *Brassica napus* after infection by *Leptosphaeria maculans*. *Journal of General Plant Pathology* **74**: 120–124.

Lindahl BD, Olsson S. 2004. Fungal translocation – creating and responding to environmental heterogeneity. *Mycologist* **18**: 79–88.

Lumsden RD. 1979. Histology and physiology of pathogenesis in plant diseases caused by *Sclerotinia* species. *Phytopathology* **69**: 890–896.

Lumsden RD, Dow RL. 1973. Histopathology of *Sclerotinia sclerotiorum* infection of bean. *Canadian Journal of Botany* **63**: 708–715.

Mei J, Ding Y, Lu K, *et al.* 2012. Identification of genomic regions involved in resistance against *Sclerotinia sclerotiorum* from wild *Brassica oleracea*. *Theoretical and Applied Genetics* **126**: 549–556.

Morrall RAA, Dueck J. 1982. Epidemiology of sclerotinia stem rot of rapeseed in Saskatchewan. *Canadian Journal of Plant Pathology* **4**: 161–168.

Nicholson RL, Hammerschimdt R. 1992. Phenolic compounds and their role in disease resistance. *Annual Review of Phytopathology* **30**: 369–389.

Prior GD, Owen JH. 1964. Pathological anatomy of *Sclerotinia trifoliorum* on clover and alfalfa. *Phytopathology* **54**: 784–787.

Rietz S, Bernsdorff F, Cai D. 2012. Members of the germin-like protein family in *Brassica napus* are candidates for the initiation of an oxidative burst that impedes pathogenesis of *Sclerotinia sclerotiorum*. *Journal of Experimental Botany* **63**: 5507–5519.

Rodríguez MA, Venedikian N, Bazzalo ME, Godeas A. 2004. Histopathology of *Sclerotinia sclerotiorum* attack on flower parts of *Helianthus annuus* heads in tolerant and susceptible varieties. *Mycopathologia* **157**: 291–302.

Sutton DC, Deverall BJ. 1984. Phytoalexin accumulation during infection of bean and soybean by ascospores and mycelium of *Sclerotinia sclerotiorum*. *Plant Pathology* **33**: 377–383.

Sylvester-Bradley R, Makepeace RJ. 1984. A code for stages of development in oilseed rape (*Brassica napus* L.). *Aspects of Applied Biology* **6**: 399–419.

Tariq VN, Jeffries P. 1984. Appressorium formation by *Sclerotinia sclerotiorum*: scanning electron microscopy. *Transactions of the British Mycological Society* **82**: 645–651.

Tariq VN, Jeffries P. 1986. Ultrastructure of penetration of *Phaseolus* spp. by *Sclerotinia sclerotiorum*. *Canadian Journal of Botany* **64**: 2909–2915.

Taylor A, Coventry E, Jones JE, Clarkson JP. 2015. Resistance to a highly aggressive isolate of *Sclerotinia sclerotiorum* in a *Brassica napus* diversity set. *Plant Pathology* **64**: 932–940.

Ulloa M, Hanlin RT. 2000. *Illustrated dictionary of mycology*. St Paul, MN: APS Press.

Uloth MB, You MP, Finnegan PM, *et al.* 2013*a*. New sources of resistance to *Sclerotinia sclerotiorum* for crucifer crops. *Field Crops Research* **154**: 40–52.

Uloth MB, You MP, Finnegan PM, Banga SS, Yi H, Barbetti MJ. 2013*b*. Seedling resistance to *Sclerotinia sclerotiorum* as expressed across diverse cruciferous species. *Plant Disease* **98**: 184–190.

Uloth MB, Clode P, You MP, Barbetti MJ. 2015*a*. Calcium oxalate crystals: an integral component of the *Sclerotinia sclerotiorum*/*Brassica carinata* pathosystem. *PLoS One* **10**: e0122362.

Uloth MB, You MP, Cawthray G, Barbetti MJ. 2015*b*. Temperature adaptation in isolates of *Sclerotinia sclerotiorum* affects their ability to infect *Brassica carinata*. *Plant Pathology*, doi:10.1111/ppa.12338.

Vance CP, Kirk TK, Sherwood RT. 1980. Lignification as a mechanism of disease resistance. *Annual Review of Phytopathology* **18**: 259–288.

Wang Z, Mao H, Dong C, *et al.* 2009. Overexpression of *Brassica napus* MPK4 enhances resistance to *Sclerotinia sclerotiorum* in oilseed rape. *Molecular Plant-Microbe Interactions* **22**: 235–244.

Wang Z, Fang H, Chen Y, *et al.* 2014. Overexpression of BnWRKY33 in oilseed rape enhances resistance to *Sclerotinia sclerotiorum*. *Molecular Plant Pathology* **15**: 677–689.

Wilcoxson RD, Subbarayudu S. 1968. Translocation to and accumulation of phosphorus-32 in sclerotia of *Sclerotium rolfsii*. *Canadian Journal of Botany* **46**: 85–88.

Williams B, Kabbage M, Kim HJ, Britt R, Dickman MB. 2011. Tipping the balance: *Sclerotinia sclerotiorum* secreted oxalic acid suppresses host defenses by manipulating the host redox environment. *PLoS Pathogens* **7**: e1002107.

Wu J, Cai G, Tu J, *et al.* 2013. Identification of QTLs for resistance to Sclerotinia Stem Rot and *BnaC.IGMT5.a* as a candidate gene of the major resistant QTL *SRC6* in *Brassica napus*. *PLoS ONE* **8**: e67740.

Zhao J, Udall J, Quijada P, Grau CR, Meng J, Osborn T. 2006. Quantitative trait loci for resistance to *Sclerotinia sclerotiorum* and its association with a homeologous non-reciprocal transposition in *Brassica napus* L. *Theoretical and Applied Genetics* **112**: 509–516.

Zhao J, Wang J, An L, *et al.* 2007. Analysis of gene expression profiles in response to *Sclerotinia sclerotiorum* in *Brassica napus*. *Planta* **227**: 13–24.

Zhao J, Buchwaldt L, Rimmer SR, *et al.* 2009. Patterns of differential gene expression in *Brassica napus* cultivars infected with *Sclerotinia sclerotiorum*. *Molecular Plant Pathology* **10**: 635–649.